

## Self-similar magnetic structures during the vortex-glass to vortex-liquid transition of type II superconductors

I. B. Krasnyuk

*A. A. Galkin Institute of Physics and Technology, National Academy of Sciences of Ukraine,  
ul. R. Lyuksemburg 72, Donetsk 83114, Ukraine*

R. M. Taranets

*Institute of Applied Mathematics and Mechanics, National Academy of Sciences of Ukraine,  
ul. R. Lyuksemburg 74, Donetsk 83114, Ukraine*

V. M. Yurchenko<sup>a)</sup>

*A. A. Galkin Institute of Physics and Technology, National Academy of Sciences of Ukraine,  
ul. R. Lyuksemburg 72, Donetsk 83114, Ukraine*

(Submitted July 12, 2010; revised September 23, 2010)

Fiz. Nizk. Temp. **37**, 369–376 (April 2011)

We examine the response to an external magnetic field by a multi-layer superconductor with an electrical resistance  $\rho_{ff}(b)\propto b^\sigma$ , where  $b$  is the dimensionless magnetic induction and  $\sigma$  is a parameter characterizing the ratio of the pinning activation energy to the energy of thermal fluctuations. When  $\sigma > 1$  the sample is in the vortex glass phase, when  $0 < \sigma < 1$ , it is in the vortex liquid phase, and a vortex glass to vortex liquid phase transition takes place at  $\sigma = 1$ . In the vortex glass phase, the magnetic field penetrates into the superconductor in the form of a self-similar wave. At all times it penetrates to a finite depth and its front moves at a finite velocity which depends on the parameters of the problem, such as the rate of pumping by the external magnetic field. In the vortex liquid phase the magnetic field penetrates to an infinite depth. Thus, the magnetic field penetrates to an infinite depth in the superconductor during a transition from the vortex glass phase into the vortex liquid phase. © 2011 American Institute of Physics. [doi: 10.1063/1.3592212]

### I. INTRODUCTION

We consider a mathematical model that can be used to explain the interaction of dynamically induced vortex instabilities in an amorphous multilayer superconductor with a single layer of Ta-Ge alloy. We shall determine the critical velocity of the vortices according to a Larkin-Ovchinnikov model.<sup>1</sup> A weak dependence of the critical vortex velocity  $v^*(H)$  on the magnetic field strength  $H$  is observed experimentally.<sup>2</sup> In fact the function  $v^*(H)$  falls off with increasing  $H$  until  $H = H_g$ , which corresponds to melting of the vortex glass. Thus, the critical velocity  $v = v^*$  is essentially independent of the field only when  $H > H_g$ .

This means that the pinning force  $F_p = F_p(v)$  is a function of the velocity of the vortices, which are in a phase similar to vortex glass when  $v < v_c$  while the system transforms into a “plastic” mass, similar to a vortex liquid phase when  $v > v_c$ .<sup>2–4</sup> With increasing velocity, as  $v \rightarrow v_c$ , the pinning force and the viscous force increase while the vortex lattice moves as a “unified whole,” i.e., we have an analog of vortex motion driven by collective pinning. When  $v > v_c$  the interaction among the vortices, the pinning force, and the viscosity are sharply attenuated, so that the vortex motion comes to resemble a plastic deformation of the vortex lattice. The corresponding shear moduli become rather small, i.e., they satisfy the Lindeman criterion for melting of a vortex lattice<sup>5</sup> and the “solid” phase for  $v < v_c$  transforms to the “plastic” high-temperature superconductor phase when  $v > v_c$ . This happens when  $B = B_m(T)$  and the resistance of the superconductor varies as shown in Fig. 1. Figure 1 is a plot of the

electrical resistance ( $E/J$ ) and the smooth line shows the resistance function predicted by the Bardeen-Stefan law,

$$\rho_{ff} = \rho_n B/H_{c2}. \quad (1)$$

Equation (1) describes free vortex motion, where  $\rho_n$  is the specific resistance in the normal phase,  $H_{c2}$  is the second critical field, and  $B$  is the magnetic induction averaged over the lattice. The deviation from free vortex motion in low fields may be caused by pinning (even at high transport

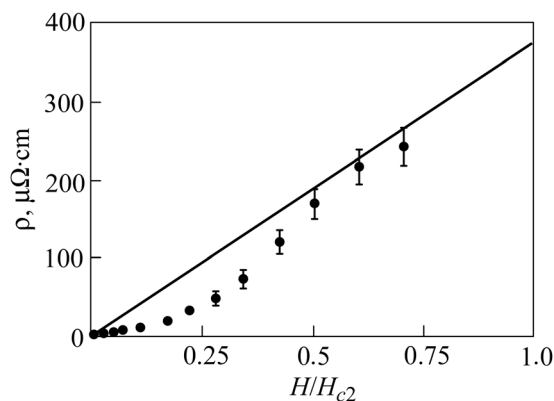


FIG. 1. Electrical resistance of a multilayer sample measured near (below) the transition to the normal state for a current density  $J = J^*$ . Even at such high transport current densities the resistance in the phase of free vortex motion (smooth line) gives a satisfactory description of the experiment above the melting curve  $H_g(T)$  for the vortex lattice; this demonstrates the importance of the “disorder” caused by pinning and/or thermal fluctuations.

current densities). In that situation, we assume that the pinning force is given by  $F_p = c(B)f(v)$ , where  $c(B)$  is a function of  $B$  and  $f(v)$  is a monotonically increasing function. An instability develops when the force opposing the motion of the vortices (viscosity and pinning forces) reaches a maximum as a function of the vortex velocity.  $c(B)$  approaches zero in the liquid phase. Then the pinning force (or the vortex velocity) is averaged over the all thermal fluctuations.  $c(B)$  reaches a maximum at low fields, where the vortices are subjected to the random pinning potential. Thus, the instability depends on the vortex velocity, the resistance to the vortex motion, and the magnetic induction.

Recall that thermal fluctuations affect the behavior of a vortex system. Vortex lines can move as a result of thermally activated “jumps” through pinning barriers even for transport currents  $J < J_c$ , which leads to so-called flow creep.<sup>6</sup> Creep is equivalent to a slight directed motion of the vortex lines. Does dissipation (and, therefore, the resistance) vanish as  $J \rightarrow 0$  or does the superconductor stay in a mixed or resistive state? The response of the system depends on the state of the superconductor:

- (1) near the melting line  $T < T_m$ , a vortex glass state exists where the pinning barrier  $U(j \rightarrow 0) \rightarrow \infty$ , which leads to a superconducting phase with resistance  $r(j \rightarrow 0) \rightarrow 0$ ;
- (2) near the melting line  $B_m(T)$ , the finite pinning barrier which inhibits vortex motion is still fairly high ( $T \leq U_0 < \infty$ ), so that the vortex liquid stays pinned (the so-called TAFF regime). Near the second critical field  $H_{c2}(T)$ , where  $H$  is the magnetic field strength, the pinning barrier is low ( $U_0 \leq T$ ) and the vortex liquid cannot be pinned (the so-called FF regime). In the FF-regime, the resistance is given by  $\rho = (\rho_{\text{flow}}/A)\exp(-U_0/T)$ , where the parameter  $A \ll 1$  characterizes the magnitude of the  $\delta T_c$  pinning caused by randomly distributed point defects (Ref. 5, p. 1138).

Let consider vortex motion in HTSC materials (e.g., the cuprates).<sup>4</sup> Recall that HTSC can be in a phase with thermally activated motion of the magnetic flux when  $J < J_c$  (TAFF-regime), in a phase with classical flux creep, in a “gigantic” flow creep phase,<sup>7-9</sup> and in a mixed state or a Shubnikov phase when  $J > J_c$ , where a viscous flow of the magnetic flux takes place, etc.<sup>7,10</sup> We shall dwell on the HTSC state consisting of a vortex glass phase.<sup>5,11,12</sup> In the vortex glass phase, the lattice has randomly disseminated point defects, i.e., is subject to the action of a weak  $\delta T_c$ -correlated pinning.<sup>5</sup> The response of the superconductor to external perturbations in the current is more or less understood as  $j \rightarrow 0$ , where  $j = J/J_c$  and  $J_c$  is the critical current density. This is explained, in particular, by the fact that in low-temperature superconductors the effect of thermal fluctuations can be neglected in the limit of low current densities. In the high current density limit, it is necessary to include the interaction between random displacements of the vortex lattice owing to the random disposition of the pinning force and the thermal fluctuations; this situation is less understood.

The existence of a fundamental instability in multilayer Ta-Ge systems with a single alloy layer that shows up as a sudden transition of the vortex system to the normal state if the control current  $J$  reaches a critical value  $J^*$ , has been demonstrated experimentally.<sup>2</sup> A theoretical analysis of the

experimentally observed instability of the vortex system shows that when  $J < J^*$  the vortices in the solid phase move collectively, while if  $J > J^*$  plastic vortex motion takes place in a vortex liquid phase.

Let us examine how the “static disorder” effect influences the vortex motion in the solid phase assuming that the pinning force  $F_p(v)$  is a function of the vortex velocity that correctly describes the system behavior near the line where instability develops,  $T_m(B)$ . The corresponding phase diagram is shown in Fig. 2. Figures 3(a) and 3(b) show typical current-voltage characteristics for multilayer superconductors in the solid and liquid phases, respectively. These plots are the result of an experiment in which the sample was subjected to weak “disorder” such that the pinning and the inter-vortex-interaction correlation length are sufficiently small.<sup>5</sup> The layered nature of the sample also leads to a deformation of the vortex lattice,<sup>5</sup> so that, for example, in the 3D limit the diameter  $l_c$  of a “vortex tube” consisting of a vortex bundle (with collective pinning) is less than the sample thickness.<sup>2-4</sup>

Note that in the vortex glass phase, the following scaling holds:<sup>2</sup>

$$\bar{E} = (E/J)[1 - T/T_g]^{v(d-2-z)}, \quad (2)$$

$$\bar{J} = J[1 - T/T_g]^{v(1-d)}, \quad (3)$$

where  $v$  and  $z$  are parameters (e.g.,  $z = 6.0 \pm 0.5$  and  $v = 1.2 \pm 0.1$ ),  $d$  is the dimensionality of the system,  $T_g$  is the vortex glass to vortex liquid transition temperature, and  $E$  is the electric field. (In general,  $v = v(B)$  depends in oscillatory fashion on the amplitude of the magnetic induction.) As an example, for a layered Ta-Ge superconductor the parameters  $z$  and  $v$  are the same for temperatures and magnetic fields. The melting curve for the vortex glass is indicated in Fig. 3(c).

A scaling analysis shows that, in the limit of low currents, the vortex glass model provides a satisfactory description of the experimental data. However, below the melting

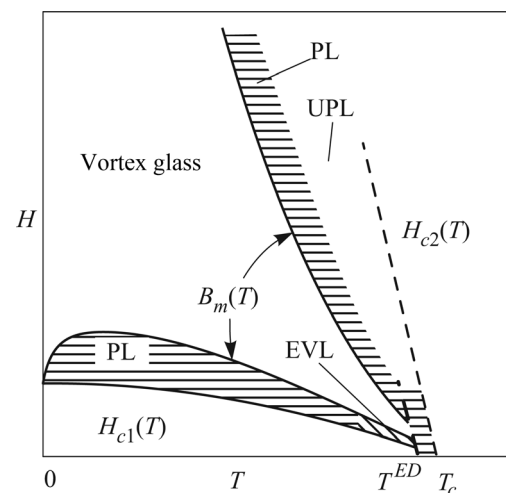


FIG. 2. A magnetic field strength-temperature phase diagram. Here  $B_m(T)$  is the melting curve for the vortex lattice,  $H_{c1}(T)$  is the first critical field,  $H_{c2}(T)$  is the second critical field, and  $T^{ED}$  is the temperature of the phase transition from the phase of entangled filaments in the liquid (entangled liquid phase) to the disentangled liquid phase. Near the melting curve the inequality  $T \ll U_0 < \infty$  holds, where  $U_0$  is the height of the barrier for plastic deformation. Near  $T_c$  the inequality  $U_0 \ll T$  holds in the entangled liquid phase. PL denotes the pinned liquid; UPL, the unpinned liquid; and, EVL, the entangled vortex liquid.

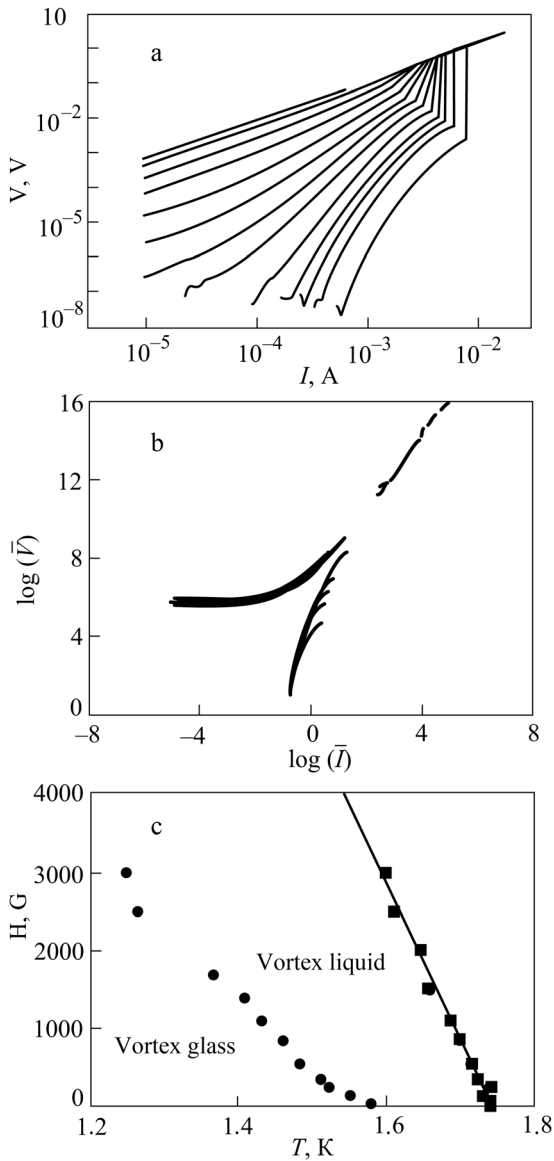


FIG. 3. (a) Current-voltage characteristics of a multilayer sample at  $T = 1.456$  K in magnetic fields (from left to right) of 40, 150, 250, 350, 550, 850, 1100, 1400, 1700, 2100, 2500, 3000,  $3500 \times 10^{-4}$  T. (b) The same curves on a logarithmic scale. (c) A phase diagram for a multilayer sample near  $T_c$ . The squares denote values of the second critical point  $H_{c2}$  and the circles, the melting curve during a vortex glass to vortex liquid phase transition.

curve at high current densities, a deviation from the scaling behavior is observed: there is a transition into the normal phase for sufficiently high current densities  $J^*$ . For curves chosen in the vortex liquid phase, there is also a transition into the normal phase. Here, as shown rigorously in Ref. 2, there is no effect from Joule heating at the point  $J = J^*$ . We explain the transitions using the classical Larkin-Ovchinnikov theory.<sup>1</sup> According to that theory, the vortex velocity is determined by the balance between the controlling Lorentz force and the vortex viscosity. Here it is important that, with a monotonic increase in the vortex velocity, the viscous force reaches a maximum at the corresponding maximum vortex velocity, and then begins to fall off, which, in turn, drives the system into a normal state, which represents a vortex glass to vortex liquid phase transition.

Figure 4 is a plot of the critical velocity  $v = v^*(H)$ . Below the transition temperature  $T_g$  the vortex lattice has finite shear moduli. The individual vortices move at some average veloc-

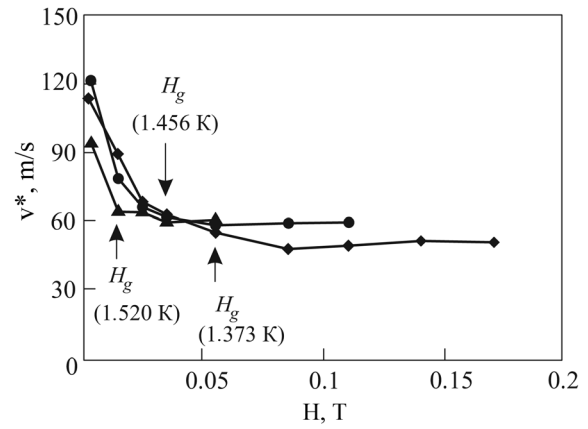


FIG. 4. Critical vortex velocity ( $v^*$ ) characterizing the Larkin-Ovchinnikov instability at 1.373 K (diamonds), 1.456 K (circles), and 1.520 K (triangles) with the corresponding melting curve ( $H_g$ ) for the vortex glass. The velocity  $v^*$  is independent of the magnetic field only above  $H_g$ .

ity. In the liquid phase (above  $T_g$ ), the shear moduli go to zero, so that the motions of the vortices become independent. Thus, there a distributions of the vortex velocity exists and the motion of each individual vortex leads to the development an instability if its velocity reaches a critical value  $v^*$ ; this leads to a “broadening” of the transition temperature  $T_g(v)$ .

## II. VORTEX LIQUID TO VORTEX GLASS PHASE TRANSITION

In this section we give an analytic description of the magnetic field perturbations during a vortex liquid to vortex glass phase transition. The equation for the evolution of the magnetic induction  $b$  is<sup>5,13–15</sup>

$$b_t = a(|b_x|^{\sigma-1} b_x)_x. \quad (4)$$

Here  $b = B/H_{c1}$  and  $a = \rho_n t_h c^2 / (4\pi\lambda^2)$  is a dimensionless magnetic field diffusion coefficient, where  $\rho_n$  is the specific resistance in the normal phase,  $t_h$  is the relaxation time for the magnetic field amplitude to an equilibrium distribution,  $c$  is the speed of light, and  $\lambda$  is the London penetration depth for the magnetic field. The parameter  $\sigma = U_0/k_B T$  characterizes the competition between the activation energy of the pinning barrier,  $U = U(j)$ , and the thermal energy  $k_B T$ . For  $\sigma > 1$ , when the thermal fluctuations are small, the vortex glass phase exists, and for  $0 < \sigma < 1$ , when the thermal fluctuations are large, the vortex liquid phase exists.  $\sigma = 1$  represents the “melting curve” in the phase diagram of Fig. 2. Note that model equations of the type (4) are a special case of the general Maxwell equations for nonlinear media.<sup>16</sup>

We seek a solution of Eq. (4) in the self-similar form,

$$b(x, t) = t^\alpha f(x/t^\beta), \quad \zeta = x/t^\beta, \quad (5)$$

where  $\alpha$  and  $\beta$  are constants and the function  $f$  is the solution to the problem,

$$\begin{aligned} \alpha f - \beta \zeta f' &= a t^{1+\alpha(\sigma-1)-\beta(1+\sigma)} (|f'|^{\sigma-1} f')', \\ f(0) &= 1, \quad f(\infty) = 0. \end{aligned} \quad (6)$$

Setting  $\beta = [1 + \alpha(\sigma - 1)]/(\sigma + 1)$ , from Eq. (6) we find

$$\alpha f - \beta \zeta f' = a (|f'|^{\sigma-1} f')'.$$

Given that  $\zeta f' = (\zeta f)' - f$ , we obtain

$$(a|f'|^{\sigma-1}f' + \beta\zeta f)' = (\alpha + \beta)f. \quad (7)$$

Let us set  $\alpha = -\beta$ ; then  $\beta = 1/2\sigma$  and  $\alpha = -1/2\sigma$ . In this case, Eq. (7) yields

$$a|f'|^{\sigma-1}f' + \beta\zeta f = C_0, \quad (8)$$

where  $C_0 = a|f'(0)|^{\sigma-1}f'(0) + K$ , provided that  $\lim_{\zeta \rightarrow 0} \zeta f(\zeta) = K < \infty$ . When  $C_0 = 0$  the solution of Eq. (8) has the form,<sup>17</sup>

$$f(\zeta) = \left[ C_1 - \frac{\sigma-1}{\sigma} \left( \frac{1}{2a\sigma} \right)^{\frac{1}{\sigma}} |\zeta|^{\frac{\sigma+1}{\sigma}} \right]^{\frac{\sigma}{\sigma-1}}, \quad \sigma \neq 1, \quad (9)$$

$$f(\zeta) = C_1 \exp\left(-\frac{\zeta^2}{4a}\right), \quad \sigma = 1, \quad (10)$$

where the constant  $C_1$  is found from the conservation of mass,  $\int f(\zeta)d\zeta = M$ . Figure 5 shows plots of  $f(\zeta)$  for the vortex glass phase ( $\sigma > 1$ ) and Fig. 6, for the vortex liquid phase ( $0 < \sigma < 1$ ). For  $\sigma > 1$  the carrier of the solution is localized and expands with the passage of time. For  $0 < \sigma < 1$  the solutions are no longer localized, but fall off with increasing  $\zeta$ . On passing through  $\sigma = 1$ , a vortex glass to vortex liquid phase transition takes place. Note that the solution (10) can be obtained as the limit of Eq. (9) as  $\sigma \rightarrow 1$ . Thus, continuity of the solution (9) ( $f \sim |\zeta|^{-(\sigma+1)/(1-\sigma)}$  for  $0 < \sigma < 1$  and  $f \sim |\zeta|^{(\sigma+1)/(\sigma-1)}$  for  $\sigma > 1$ ) depends significantly on the value of  $\sigma$  and breaks down on passing through  $\sigma = 1$ , which is indicative of a phase transition.

In the case  $\sigma > 1$  the velocity of the wave front is

$$v_{\{\sigma > 1\}} = C_2 t^{\frac{1-2\sigma}{2\sigma}}, \quad \text{where } C_2 = \left[ \frac{C_1 a^{1/\sigma}}{2(\sigma-1)} \right]^{\frac{\sigma}{\sigma+1}}. \quad (11)$$

As opposed to the previous case, for  $\sigma \leq 1$  we can only determine an effective velocity of the wave front,

$$v_{\{\sigma \leq 1\}} = \zeta_{\text{eff}} t^{\frac{1-2\sigma}{2\sigma}} \quad (12)$$

where  $\zeta_{\text{eff}}$  is found using the condition  $f(\zeta_{\text{eff}}) = 1/2$ , i.e.,  $\zeta_{\text{eff}} = f^{-1}(1/2)$ . Equations (11) and (12) imply that the front

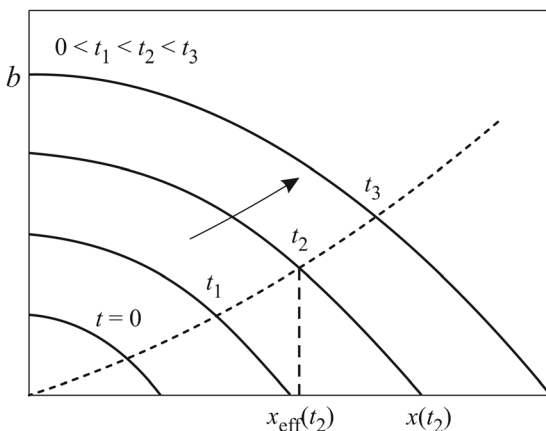


FIG. 5. Penetration of the magnetic wave front and its amplitude in the vortex glass regime ( $\sigma > 1$ ).

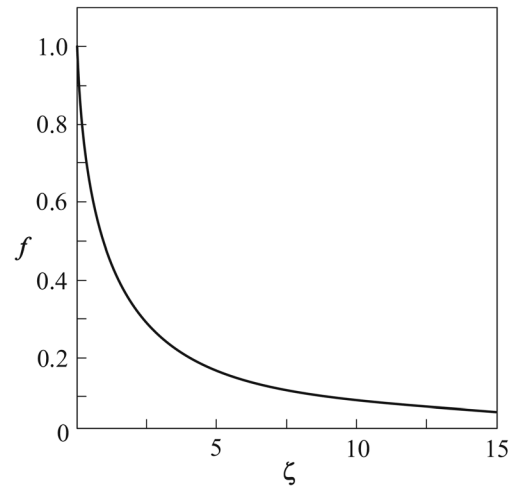


FIG. 6. Distribution of magnetic perturbations in the pinned vortex liquid phase ( $1/2 < \sigma < 1$ ).

velocity decreases with the passage of time if  $\sigma > 1/2$ . When  $\sigma = 1/2$  the velocity becomes constant and for  $0 < \sigma < 1/2$ , the superconductor enters the normal state.

Let us check the magnetic flux creep condition  $0 < j = -kb_x < 1$  for the case of  $\sigma = 1$ , where  $k = cH_{c1}/(4\pi J_c \lambda)$ . A direct calculation shows that in this case,

$$j = \frac{H_{c1} \lambda C_1}{2J_c \rho_n t_h c} \frac{|x|}{t^{3/2}} \exp\left(-\frac{x^2}{4at}\right)$$

and the condition  $j < 1$  is satisfied within the region  $|x| < [2J_c \rho_n t_h c / H_{c1} \lambda C_1] t^{3/2}$ . Given this and Eq. (12), it is evident that the region of effective localization is contained within the region  $j < 1$  for any  $t \geq t^*$ , where

$$t^* = \frac{H_{c1} \lambda C_1 \zeta_{\text{eff}}}{J_c \rho_n t_h c} \zeta_{\text{eff}} = 2\sqrt{a \ln(2C_1)}, \quad C_1 = \frac{M}{2\sqrt{\pi a}}.$$

### III. DESCRIPTION OF EXPERIMENT

The resistance and current-voltage characteristic of the mixed phase of  $\text{Ta}_x\text{Ge}_{1-x}/\text{Ge}$  films were measured in the experiment of Ref. 2 for three films with different coupling between the layers and correlation defects. The experimental data are analyzed in terms of a model of vortex glass and a phase transition from a resistive vortex liquid to an immobilized glass-like phase.

Amorphous multilayer films were prepared by deposition (see Fig. 7) on a glass substrate. Layering is done by periodic placing of a barrier in front of the flux of Ta vapor. An inclination of the substrate relative to the vapor flux leads to the formation of a columnar structure with regions of lower density between the columns. The average size of the columns is on the order of 100 nm. Note that, in the experiment, the first two films have a strong Josephson contact between neighboring layers: the layers of germanium had a thickness of less than 5 nm (above that the Josephson contact becomes weak; the third film).

A mixed state of two  $\text{Ta}_{0.3}\text{Ge}_{0.7}/\text{Ge}$  layers was examined in the experiment. There could be several or just one of these layers. Thus, the sample consists of several monolayers of TaGe alloy and pure Ge fabricated in the form of an

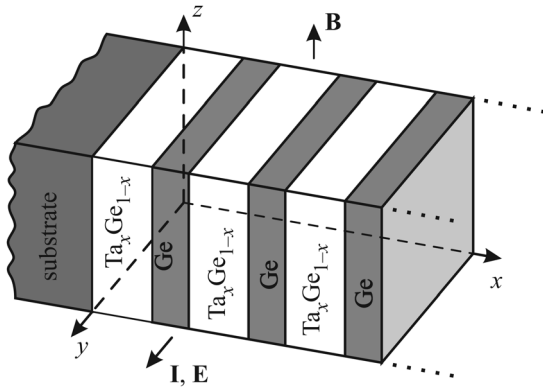


FIG. 7. The geometrical arrangement for the measurements. The transport current  $J_y$  is parallel to the film and perpendicular to the microstructure and to the magnetic field vector  $B_z$ .

amorphous layer on the glass substrate.<sup>2</sup> The film is stable even far above room temperature.<sup>21</sup> The composition of the alternating superconducting layers of  $Ta_{0.3}Ge_{0.7}$  is diluted by the semiconducting Ge, which serves as an insulator. The critical temperature for a single layer of the alloy with 30% Ta is  $T_c = 2.9$  K.<sup>3,18</sup> A multilayer sandwich sample has a thickness of  $1250 \text{ \AA}$  and 25 layers consisting of pairs of Ga ( $25 \text{ \AA}$ ) and Ta ( $25 \text{ \AA}$ ) and a single  $600\text{-\AA}$ -thick layer of the alloy.<sup>2</sup>

Each of the layers has a low critical temperature  $T_c = 1.7$  K that is determined by the coupling between the thin superconducting layers and the existence of the alloy layer with a surface layer that has a higher temperature  $T_c'$  compared to the individual  $T_c$  of the layers. The sample manifests an instability (induced by a change in the current density) of the vortex system in accordance with the Larkin-Ovchinnikov theory.<sup>1</sup> The instability arises in the Ta-Ge monolayer system and in the lone alloy layer, which is the reason for the appearance of the transition jump of the superconductor into the normal phase when the control current exceeds some critical value. The instability arises as a transition from collective motion of the vortices in the rigid vortex lattice to plastic motion of the vortices in the vortex liquid phase. Here the pinning force is a function of the vortex velocity near the instability region. The rf complex resistance (at 75 MHz) of an oxygen-doped aluminum film perforated by a triangular lattice of  $1\text{-}\mu\text{m}$ -diam "holes"  $3 \mu\text{m}$  part, has been measured<sup>4</sup> as a function of temperature and magnetic field. This structure was chosen in order to obtain subcritical "hole-hole" coupling forces. The coupling constant of the pinning force was measured and could be used to determine the localized vortex "instabilities," consisting of a cluster of vortices located between "holes." The phenomenological equation of motion has the form,

$$\eta x' + kx = J\phi_0/c, \quad (13)$$

where  $x$  is the coordinate of the vortex density at time  $t > 0$ , the parameter  $k$  models the averaged pinning force,  $\eta$  is the viscosity,  $J$  is the density of the applied transport current, and  $\phi_0$  is the quantum of magnetic flux. The formula  $E = x'B/c$  for the electric field implies that

$$\Re[\rho] = \rho f \cos^2 \phi \quad (14)$$

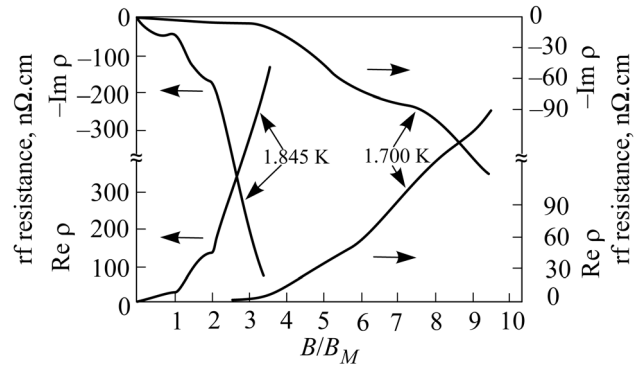


FIG. 8. The real and imaginary components of the rf resistance measured at 75 MHz as functions of the normalized magnetic field.  $T_c = 1.875$  K,  $B_M = 2.76$ , and the Ginzburg-Landau parameter  $\kappa = 11$ .

$$\Im[\rho] = B\phi_0 \sin 2\phi/kc^2, \quad (15)$$

where  $\rho f = B\phi_0/\eta c^2$  is the resistance in the viscous flow regime,  $\tau = \eta/k$  is the relaxation time for the vortex lattice to its equilibrium position, and  $\phi = \text{ctg}^{-1} \omega\tau$  is the phase angle. Figure 8 shows graphs of the two components of the complex rf resistance as functions of the magnetic field  $B$  normalized to the field  $B_M$  at which the flux density equals the density of "holes." At  $T = 1.7$  K the rf resistance starts to increase when  $B_{th} = 3B_M$ . The critical field  $B_{th}$  increases monotonically as the temperature is reduced. Figure 8 shows that the real part of the resistance can actually be approximated by a power law dependence. It has been shown<sup>4</sup> that  $\omega\tau \sim 1$  in the magnetic field region for  $T = 1.7$  K. However,  $\Im[\rho] > \Re[\rho]$  when  $B = B_{th}$ . Here the resistance  $\rho f$ , defined in accord with Eq. (15), increases with magnetic field for  $B > B_{th}$ . A similar result was obtained at lower temperatures. These results can be interpreted for  $B < B_{th}$  as the complete capture of the magnetic flux by the "holes." For  $B > B_{th}$ , an additional flux is created by the vortex localized states lying between the "holes" and coupled by pinning centers.

#### IV. CONCLUSION

A mathematical model has been proposed to describe the magnetic perturbations in the current-voltage characteristics, whose curvature changes in the neighborhood of some temperature  $T_g$ , which can be interpreted as a phase transition. It has been shown that this model provides an adequate description of the evolution of self-similar magnetic perturbations during a vortex glass to vortex liquid phase transition.<sup>19</sup> In addition, this model, represented by a special diffusion equation of the gradient type (first obtained in Ref. 5), can describe the structure of the vortex lattice in other phases with pinning taken into account, and not only for weak collective pinning, e.g., taking a sinusoidal pinning potential into account for the model discussed in Ref. 20. In particular, for the model of a vortex glass to vortex liquid phase transition,  $T_g$  is the temperature of the phase transition from a viscous vortex flow to flow creep within a specified range of stresses.<sup>20</sup>

We have limited ourselves to a mathematical study of possible self-similar perturbations of the magnetic induction in a multilayer Ta-Ge superconductor with a single alloy layer<sup>2</sup> where the electrical resistance is an exponential function of the magnetic induction,  $\rho_{ff}(b) = \rho_n b^\sigma$ ,  $\sigma > 0$ . The parameter  $\sigma \sim U_0/k_B T$  describes the effect of the activation

barrier and thermal fluctuations. When  $\sigma > 1$  the vortex glass phase is always pinned by collective weak  $\delta T_c$  pinning. On passing through  $\sigma = 1$ , the vortex lattice loses its rigidity; this leads to a phase transition when can be a vortex glass to vortex liquid phase transition at  $T_g$  or a phase transition of another type (see Fig. 8). When  $0 < \sigma < 1$  the vortex lattice loses its rigidity, but still cannot be pinned, i.e., it is subject to plastic deformation. The pinning decreases until magnetic fields  $B = B_{\text{dep}}$  within the interval  $B_m < B_{\text{dep}} < B$ , where  $B_{\text{dep}}$  is the depinning field. When  $B > B_{\text{dep}}$ , the velocity (and amplitude) of the self-similar magnetic wave increases, so that the superconductor undergoes a transition to the normal state.

<sup>a)</sup>Email: yurch@yurch.fti.ac.donetsk.ua

<sup>1</sup>A. D. Larkin and Yu. N. Ovchinnikov, Zh. Éksp. Teor. Fiz. **31**, 1915 (1975).

<sup>2</sup>B. J. Ruck, J. C. Abele, and H. J. Trodahl, Phys. Rev. Lett. **78**, 3378 (1997).

<sup>3</sup>H. J. Trodahl, H. L. Johnson, A. B. Kaiser, C. K. Subramaniam, B. J. Ruck, and P. Lynam, Phys. Rev. B **53**, 15226 (1996).

<sup>4</sup>A. T. Fiory, A. F. Hebard, and R. P. Minnich, J. Phys. **39**, C6 633 (1978).

<sup>5</sup>G. B. Blatter, M. V. Feigel'man, V. B. Geshkenbein, and A. I. Larkin, Rev. Mod. Phys. **66**, 1125 (1994).

<sup>6</sup>P. W. Anderson, Phys. Rev. Lett. **9**, 309 (1962).

<sup>7</sup>A. Campbell and J. Evetts, *Critical Currents in Superconductors* [Russian translation] (Mir, Moscow, 1975).

<sup>8</sup>I. B. Krasnyuk and R. M. Taranets, Zh. Tekh. Fiz. **77**(10), 1 (2007).

<sup>9</sup>I. B. Krasnyuk, Zh. Tekh. Fiz. **77**(5), 30 (2007).

<sup>10</sup>I. B. Krasnyuk and Yu. V. Medvedev, Zh. Tekh. Fiz. **73**(12), 31 (2003).

<sup>11</sup>M. P. A. Fisher, Phys. Rev. Lett. **62**, 1425 (1989).

<sup>12</sup>D. S. Fisher, M. P. A. Fisher, and D. A. Huse, Phys. Rev. B **43**, 130 (1991).

<sup>13</sup>I. B. Krasnyuk and M. V. Zalutskii, Fiz. Nizk. Temp. **33**, 416 (2007) [Low Temp. Phys. **33**, 307 (2007)].

<sup>14</sup>I. B. Krasnyuk and Yu. V. Medvedev, Pis'ma v Zh. Tekh. Fiz. **31**(10), 40 (2005).

<sup>15</sup>I. B. Krasnyuk and R. M. Taranets, Zh. Tekh. Fiz. **78**(8), 83 (2008).

<sup>16</sup>Yu. V. Namlyeyeva, R. M. Taranets, and V. M. Yurchenko, FTVD **19**(4), 44 (2009).

<sup>17</sup>A. A. Samarskii, V. A. Galaktionov, S. P. Kurdyumov, and A. P. Mikhailov, *Blow-up in Quasi-Linear Parabolic Equations* [Russian translation] (Nauka, Moscow, 1987).

<sup>18</sup>A. Engel, H. J. Trodahl, J. C. Abele, and S. M. Robinson, Phys. Rev. B **63**, 184502 (2001).

<sup>19</sup>R. H. Koch, V. Foglietti, W. J. Gallagher, G. Coren, A. Gupta, and M. P. A. Fisher, Phys. Rev. Lett. **63**, 1151 (1989).

<sup>20</sup>A. N. Lykov and A. Yu. Tsvetkov, Fiz. Tverd. Tela (St. Petersburg) **40**, 989 (1998).

<sup>21</sup>S. Kumer and H. J. Trodahl, J. Appl. Phys. **73**, 1761 (1993).

Translated by D. H. McNeill